Digital Linearization of Direct-Detection Transceivers for Spectrally Efficient 100 Gb/s/λ WDM Metro Networking

Zhe Li, *Student Member, IEEE*, M. Sezer Erkılınç, Kai Shi, *Member, IEEE*, Eric Sillekens, *Student Member, IEEE*, Lidia Galdino, *Member, IEEE*, Tianhua Xu, *Member, IEEE*, Benn C. Thomsen, *Member, IEEE*, Polina Bayvel, *Fellow, IEEE*, and Robert I. Killey, *Senior Member, IEEE*

(Corning Student Award Winner)

***Abstract*—Single-polarization, single-photodiode-based direct-detection (DD) transceivers offer advantages for metro networks due to their simple and low-cost optical hardware structure. Single-sideband Nyquist-pulse-shaped subcarrier modulation (SSB Nyquist-SCM) is a promising signal format to achieve high information spectral density (ISD) in such DD systems. In this paper, we present theoretical and experimental evaluations of a variety of direct-detection SSB Nyquist-SCM system designs, operating at 100 Gb/s per wavelength in wavelength division multiplexing (WDM) metro network scenarios. Through simulations, several receiver-based digital linearization techniques to overcome the effect of signal-signal beat interference were investigated, and their performance compared with alternative approaches, including optical beat-interference cancellation receivers (BICRx) and coherent receivers (both heterodyne and homodyne). Subsequently, experimental assessments of the digitally-linearized DD receivers were carried out. Spectrally efficient (net ISD exceeding 3 b/s/Hz) 4 × 112 Gb/s WDM DD single-sideband 16-QAM Nyquist-SCM transmission over distances of up to 240 km (multi-span links) and 160 km (single-span links without mid-span amplification) were shown to be possible using uncompensated standard single-mode fiber.**

***Index Terms*—Digital linearization, direct detection, Kramers-Kronig receiver, metro networks, Nyquist-pulse shaped subcarrier modulation, receiver-based electronic dispersion compensation, signal-signal beat interference, spectrally-efficient wavelength division multiplexing.**

Manuscript received June 30, 2017; revised October 18, 2017 and November 16, 2017; accepted November 16, 2017. Date of publication November 26, 2017; date of current version February 24, 2018. This work was supported by the UK Engineering and Physical Sciences Research Council UNLOC EP/J017582/1 Project. *(Corresponding author: Zhe Li.)*

Z. Li, M. S. Erkılınç, E. Sillekens, L. Galdino, P. Bayvel, and R. I. Killey are with the Optical Networks Group, Department of Electronic and Electrical Engineering, University College London, London WC1E 7JE, U.K. (e-mail: zhe.li@ee.ucl.ac.uk; m.erkilinc@ee.ucl.ac.uk; e.sillekens@ee.ucl.ac.uk; l.galdino@ee.ucl.ac.uk; p.bayvel@ucl.ac.uk; r.killey@ucl.ac.uk).

K. Shi and B. C. Thomsen are with Microsoft Research, Ltd., Cambridge CB1 2FB, U.K. (e-mail: t-kashi@microsoft.com; benn.thomsen@microsoft.com).

T. Xu is with the School of Engineering, University of Warwick, Coventry CV4 7AL, U.K. (e-mail: tianhua.xu@warwick.ac.uk).

Color versions of one or more of the figures in this paper are available online at http://ieeexplore.ieee.org.

Digital Object Identifier 10.1109/JLT.2017.2777858

I. Introduction

METRO networks are experiencing unprecedented traffic growth. The provision of bandwidth-intensive high-performance computing, information and entertainment, supported by cloud services, broadband video and mobile technologies are creating a rapidly increasing demand for high capacity optical links. A recent forecast has indicated that metro traffic volume is growing almost twice as rapidly as the traffic traversing the backbone networks and that, in the near future, 75% of the world's data traffic will be terminated within metro networks [1]. Although wavelength division multiplexing (WDM) is commonly used in metro transport networks to provide significant capacity gains over single-channel systems, it is expected that, to cope with the ever-increasing traffic growth, higher data rates (100 Gb/s and above) per WDM channel will need to be deployed [2].

Due to the cost-sensitive nature of metro networks, it may be favorable to utilize single-polarization, single-photodetector direct-detection (DD) transceivers because of the lower complexity and cost of their optical hardware structures in comparison to polarization-multiplexing coherent transceivers [3], [4]. Single-sideband subcarrier modulation (SCM) schemes, such as orthogonal frequency division multiplexing and single-subcarrier Nyquist pulse-shaped modulation with high-order quadrature amplitude modulation (QAM) potentially offer high information spectral densities. However, the performance of conventional DD SCM systems is severely degraded because of the nonlinear effect, introduced by the direct (square-law) detection in the receiver, referred to as signal-signal beat interference (SSBI). The signal-signal beating products fall within the signal bandwidth, and interfere with the wanted signal-carrier beating products.

Recently, a beating interference cancellation receiver (BICRx) has been proposed, offering superior performance [5], [6]. However, the complexity of the optical hardware in such receivers is significantly increased as they require a pair of photodiodes, an optical splitter and a very narrow optical band-stop filter (<1 GHz) to suppress the optical carrier in the received signal. Alternatively, since the SSBI products fall over a

bandwidth equal to that of the original subcarrier modulated signal (B_{sc}), a second solution to avoid the SSBI penalty is to leave a sufficient spectral guard-band ($B_{gap} \geq B_{sc}$) between the optical carrier and the subcarrier modulated signal [7], [8]. However, the drawback of this approach is that it wastes approximately 50% of the electrical and optical components' bandwidth and consequently halves the spectral efficiency. Fortunately, recently demonstrated digital linearization techniques have been shown to be effective in reducing the SSBI penalties, allowing the use of narrow or even no spectral guard-band, without requiring a change to the single photodiode-based optical hardware design [9]–[27].

Key questions concern how the performance of DD systems compares with coherent systems and whether DD systems are capable of offering high capacity transmission (100 Gb/s/λ or more) at high information spectral densities (net ISD ≥ 3 (b/s)/Hz) over WDM metro reaches (up to 300 km). To address these questions, in this paper we present theoretical and experimental performance evaluations of 100 Gb/s/λ WDM metro links utilizing DD transceivers. This paper is an extension of the work presented in [11], with additional theoretical comparisons, and in-depth descriptions of the experiments, including the optimization of the carrier-to-signal power ratio. This paper is organized as follows: Section II introduces the working principle of the recently proposed single-stage linearization filter [9], two-stage linearization filter [10] and the Kramers-Kronig scheme [12] which compensate signal-signal beating interference in DD receivers. In Section III, we describe a variety of transceiver architectures, including coherent transceivers (both homodyne and heterodyne) [28], [29] and direct-detection transceivers, employing single-sideband (SSB) Nyquist-pulse-shaped subcarrier modulation (Nyquist-SCM) and a number of different optical and digital linearization schemes. The Nyquist-SCM format, described in [30]–[34], is chosen due to its lower peak-to-average power ratio compared to orthogonal frequency division multiplexing (OFDM). We present performance comparisons between these transceivers through numerical simulations of their back-to-back operation, and demonstrate the performance/complexity tradeoff achieved with the digitally-linearized DD transceiver designs. Section IV describes our experimental setup to assess the performance of spectrally-efficient (net information spectral density of up to 3.17 (b/s)/Hz) 4 × 112 Gb/s WDM DD SSB 16-QAM Nyquist-SCM systems with receiver-based electronic dispersion compensation. In Section V, we report experimental WDM back-to-back and transmission results, including an assessment of the performance of the system over a WDM channel spacing range of 33–50 GHz and in transmission over uncompensated standard single mode fiber multiple-span links of up to 240 km and single-span links of up to 160 km.

II. Receiver-Based Digital Linearization Schemes

As mentioned in Section I, the SSBI penalty caused by square-law photodetection severely degrades the performance of DD transceivers. In order to avoid the SSBI penalty, and hence simultaneously achieve high spectral-efficiency and low optical

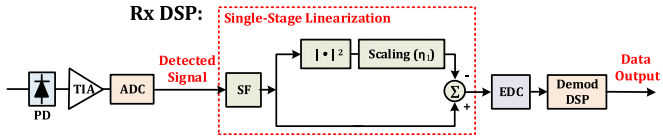

Fig. 1. Receiver DSP including single-stage linearization filter and receiver-based electronic dispersion compensation (Rx-EDC). Demod DSP: conventional demodulation DSP for SSB SCM signal. PD: photodiode, TIA: transimpedance amplifier SF: sideband filter.

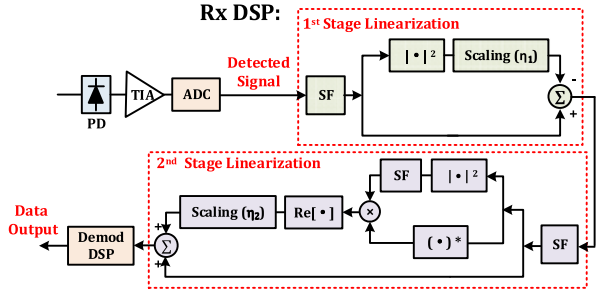

Fig. 2. Receiver DSP using the two-stage linearization filter and Rx-EDC. Demod DSP: conventional demodulation DSP for SSB SCM signal. PD: photodiode, TIA: transimpedance amplifier SF: sideband filter.

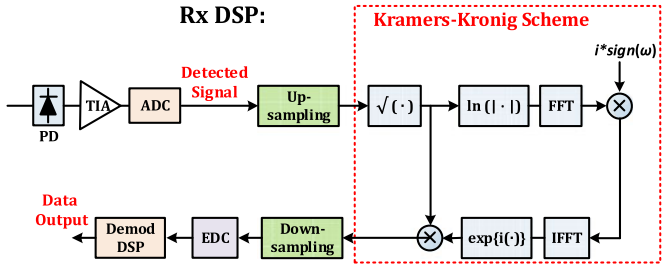

Fig. 3. Receiver DSP using the Kramers-Kronig scheme and Rx-EDC. Demod DSP: conventional demodulation DSP for SSB SCM signal.

hardware complexity, DSP-based linearization techniques, which allow the use of a narrow (or zero) spectral guardband have been proposed and demonstrated. Among the recently demonstrated digital linearization approaches, due to their advantages of either DSP algorithm simplicity or performance superiority, three digital linearization techniques are considered in this paper: a single-stage linearization filter, a two-stage linearization filter and the Kramers-Kronig scheme. The receiver DSP designs of these approaches are shown in Figs. 1–3.

The receiver-based digital single-stage and two-stage linearization filters, shown in Figs. 1 and 2, treat the SSBI terms as a perturbation to the signal. The compensation works by calculating these terms and subtracting them from the detected signal. Unlike the SSBI estimation and cancellation schemes [20], [22], [23], [26], since the calculation of the SSBI terms is carried out directly from the detected signal rather than from a reconstruction of it based on symbol decisions, the linearization filters offer significantly reduced DSP complexity, and avoid the need for accurate symbol decision making when reconstructing the beating terms. In the single-stage linearization filter (see Fig. 1) [9], a digital SSB signal is first obtained from the detected electrical signal (which is double sideband following the square law detection of the optical SSB signal) using a sideband

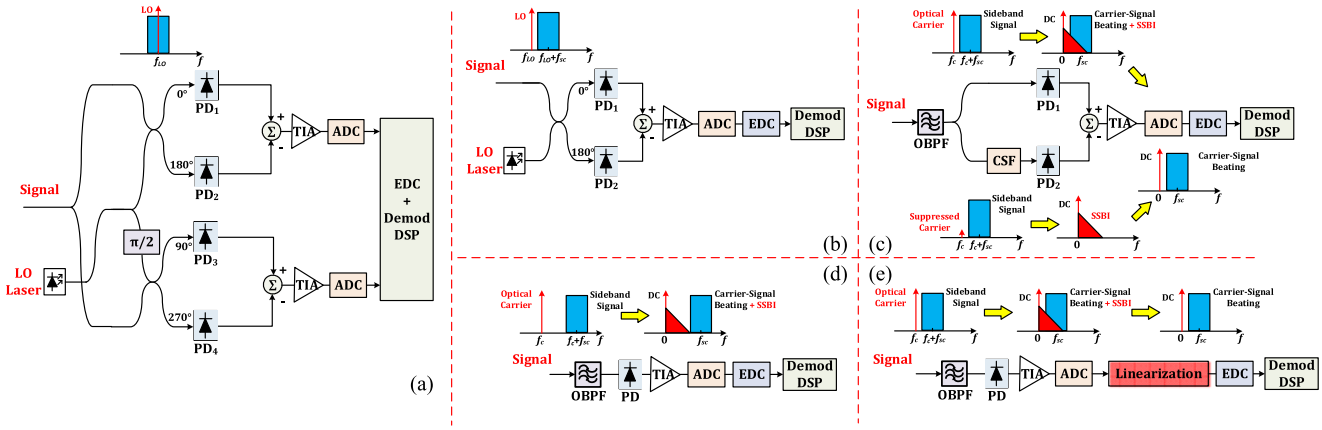

Fig. 4. Schematic diagrams of different 100 G receiver architectures. (a) Coherent homodyne, (b) coherent heterodyne, (c) beating interference cancellation receiver (BICRx), (d) DD with guard-band and (e) DD without guard-band and with digital linearization technique. OBPF: optical band-pass filter. PC: polarization controller. LO: local oscillator. CSF: carrier suppression filter. PD: photodiode. TIA: transimpedance amplifier. ADC: analogue-to-digital converter. Demod DSP: conventional demodulation DSP for baseband (coherent homodyne system) signal or SSB SCM signal (coherent heterodyne and DD systems).

filter (SF). The waveform of the SSBI terms are calculated and then subtracted from the filtered SSB signal. It can be seen that the single-stage linearization filter has very low DSP complexity, but it suffers from the problem of introducing additional unwanted beating interference by the linearization filter itself, as the calculation of the SSBI terms is based on the received distorted signal. This problem can be solved, to a large extent, by adding an extra linearization stage to compensate the majority of the beating interference introduced by the single-stage linearization filter. This latter technique, depicted in Fig. 2, is termed the two-stage linearization filter [10], [11]. The two-stage linearization offers improved performance compared to the single-stage linearization filter. At the same time, in comparison to the iterative linearization filter proposed in [21] and [32] (which is an alternative method to improve the performance of the single-stage linearization filter), the two-stage linearization technique achieves similar performance and avoids the need for multiple iterations, leading to a comparatively low DSP complexity.

Instead of treating SSBI terms as a perturbation to be removed, an alternative technique, the recently proposed and demonstrated Kramers-Kronig (KK) receiver, accurately reconstructs the optical phase of the transmitted SSB signal from its detected intensity [12]–[19], therefore recovering the waveform of the optical SSB signal. The receiver DSP is shown in Fig. 3. Provided the transmitted signal fulfils the minimum phase condition (achieved by the optical carrier having an amplitude larger than that of the signal in the sideband), and making the assumption that the optical signal is an ideal single-sideband one, the phase of the transmitted SSB signal is linked to its amplitude through the Kramers-Kronig relation [35]. Details of the KK algorithm are given in [12] and [14]. In the KK algorithm, due to the high bandwidth of the signals resulting from the square-root and logarithm operations, it is necessary for the DSP to operate at a relatively high oversampling rate. Our latest work [15] has shown that successful operation of the KK scheme can be achieved at 4 Sa/symbol, with optimum performance requiring ≥6 Sa/symbol.

From the above discussion, it can be seen that two key conditions need to be fulfilled to achieve optimum performance of the KK scheme: firstly, the transmitted SSB signal should have a sufficiently high power optical carrier, i.e., a sufficiently high carrier-to-signal power ratio (CSPR), to ensure minimum phase signaling, and, secondly, digital upsampling to deal with the bandwidth broadening effect within the KK algorithm must be implemented.

III. Performance Assessment of Different 100 G Transceiver Structures

This section presents theoretical performance comparisons of a variety of coherent and direct-detection system designs based on simulations of ideal transceivers operating at a gross bit rate of 112 Gb/s/λ. Fig. 4 shows schematic diagrams of the different receiver architectures being considered. The coherent receivers considered include conventional homodyne and heterodyne structures [28], [29] [see Fig. 4(a) and (b)], while the direct-detection receiver structures include the beating interference cancellation receiver [see Fig. 4(c)] [5], [6], and single-photodiode-based systems, firstly with a spectral guard-band sufficiently large to avoid SSBI [7], [8] [see Fig. 4(d)], and secondly with digital linearization without a spectral guard-band [see Fig. 4(e)] [9], [10], [12].

Practical limitations such as digital-to-analogue converter (DAC) and analogue-to-digital converter (ADC) quantization noise, non-negligible laser linewidths and low-pass filtering effects due to bandwidth limitations of the electrical components were neglected. Shot and thermal noise in the receivers were neglected, due to the assumption that optical amplified spontaneous emission (ASE) noise dominates. Optical band-pass filters with rectangular-shaped passbands were used to model the wavelength demultiplexer/ASE noise suppression filter, and the carrier suppression filter (CSF), used in the BICRx to completely remove the optical carrier, had a 1 MHz 3-dB bandwidth. The modulation format being used in all cases was a 28 Gbaud (112 Gb/s) 16-QAM Nyquist signal. For the coherent systems,

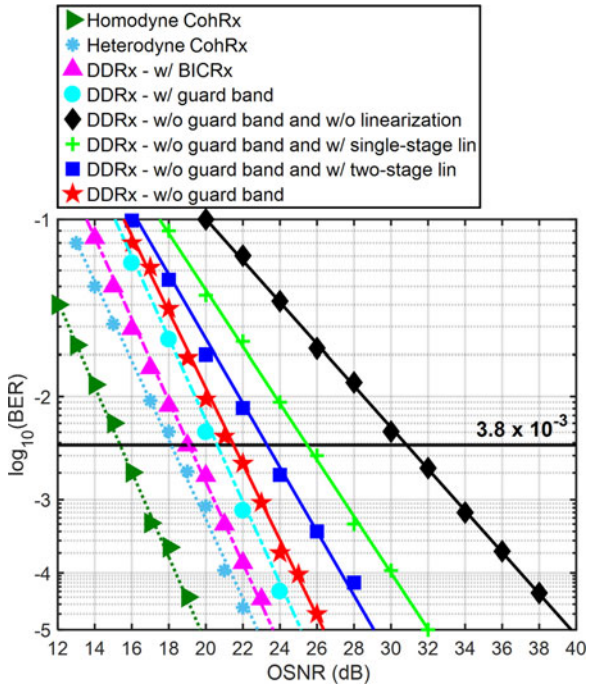

Fig. 5. Theoretical BER versus OSNR with different coherent and DD transceiver architectures.

an LO power 25 dB higher than the received signal power was used, with the LO centered on the signal in the case of the homodyne coherent receiver, and spaced 14.28 GHz away from the center of the signal in the case of heterodyne reception. The signal and LO polarizations were assumed to be perfectly aligned. The digitally-linearized DD SSB 16-QAM Nyquist-SCM receivers were 0.51 $\times$ cycle (optical carrier spaced by 14.28 GHz from the center of the QAM signal), while the DD system with the spectral guardband operated at 1.5 $\times$ cycle, hence avoiding any SSBI. In all cases, the 16QAM Nyquist signals were generated using root-raised cosine (RRC) filters with a roll-off parameter of 0.01. The digital receiver linearization techniques tested were the single- and two-stage linearization filters and the KK scheme described in the previous section. Note that a sampling rate of 6 Sa/symbol was utilized in the DSP carrying out the Kramers-Kronig algorithm, to achieve the best possible performance. The back-to-back system performance was evaluated by amplified spontaneous emission (ASE) noise loading and the bit error ratio (BER) as a function of optical signal-to-noise ratio (OSNR) is plotted in Fig. 5 for all the schemes. The numerator of the OSNR is the signal power (including both the sideband and the optical carrier power), and the denominator is the integral of the ASE noise power spectral density over the resolution bandwidth (0.1 nm). Note that, in the case of the direct-detection systems, since an optical carrier is added at the transmitter to enable the 16QAM signals to be recovered through carrier-signal beating, it is necessary to optimize the optical carrier-to-signal power ratio at each OSNR level to achieve the best performance. CSPR optimization here (and throughout the paper) was performed with the aim of minimizing the BER. (Note that the coherent results shown in this figure are for a single-polarization 112 Gb/s coherent transceiver. For a polarization-multiplexed 112 Gb/s (2 $\times$ 56 Gb/s) coherent transceiver, the information spectral density would be doubled at the same OSNR). After signal demodulation, hard decision forward error correction (HD-FEC) was assumed (due to its lower complexity and power consumption than soft decision FEC). Based on the specifications of the practical receiver design described in [36], we assume in this paper a BER threshold of 3.8×10^{-3} with a 7% overhead.

It can be seen that, between the homodyne coherent system and the DD system without guard-band and without SSBI compensation, there is a 15.7 dB difference (from 15.3 dB to 31.0 dB) in the required OSNR at the HD-FEC threshold. For the single-photodiode direct-detection receiver, the required OSNR is reduced to 25.6 dB (a 5.4 dB improvement) or 23.3 dB (a gain of 7.7 dB) by applying a single-stage linearization filter or a two-stage linearization filter, respectively. Moreover, by utilizing the KK scheme, the required OSNR is reduced further, to 21.5 dB (a 9.5 dB reduction), which is only 0.8 dB higher than that for the case of DD with sufficient spectral guard-band (1.5 $\times$ cycle SCM). Finally, with the use of the optical method to mitigate the SSBI (the BICRx), the required OSNR was found to be 19.1 dB, which is 0.9 dB higher than that with heterodyne coherent detection. This can be explained by the presence of the optical carrier with the BICRx, which is not needed in the case of coherent detection. The optical carrier-to-signal power ratio was swept, and the optimum value, for the BICRx, was found to be –6 dB at all values of OSNR. It can be observed that the performance difference between the coherent and DD systems is significantly reduced through the use of effective digital or optical receiver linearization. However, although the direct-detection system with BICRx enables reception at an OSNR only 3.8 dB higher than with the coherent homodyne system, the optical hardware complexity is significantly higher than that of the other direct-detection approaches due to the requirement of a pair of photodetectors, an optical splitter and the very narrow optical carrier suppression filter. The DD system with a spectral guard-band offers slightly poorer performance compared to the BICRx scheme, but is wasteful of spectrum. The digitally-linearized receivers, on the other hand, offer a good compromise between spectral efficiency, complexity and performance. The difference in required OSNR between the heterodyne coherent receiver and the DD receiver employing the digital KK scheme without guard-band is only 3.3 dB.

Since the optimization of CSPR is crucial for the performance of SSB SCM DD systems, further analysis of CSPR optimization and its impact on system performance was carried out by calculating optimum CSPR versus OSNR, and required OSNR (at $\mathrm{BER} = 3.8 \times 10^{-3}$) versus CSPR, both plotted in Fig 6.

For the DD system without guard-band or linearization, it can be seen from Fig. 6(a) that the optimum CSPR value increases with the OSNR; every 2 dB increase in OSNR corresponds to an increase by approximately 1 dB in the optimum CSPR value. The optimum CSPR increases from 7 dB to 16 dB over the OSNR range 18 dB to 36 dB. The increase in the optimum CSPR with increasing OSNR value can be explained as follows:

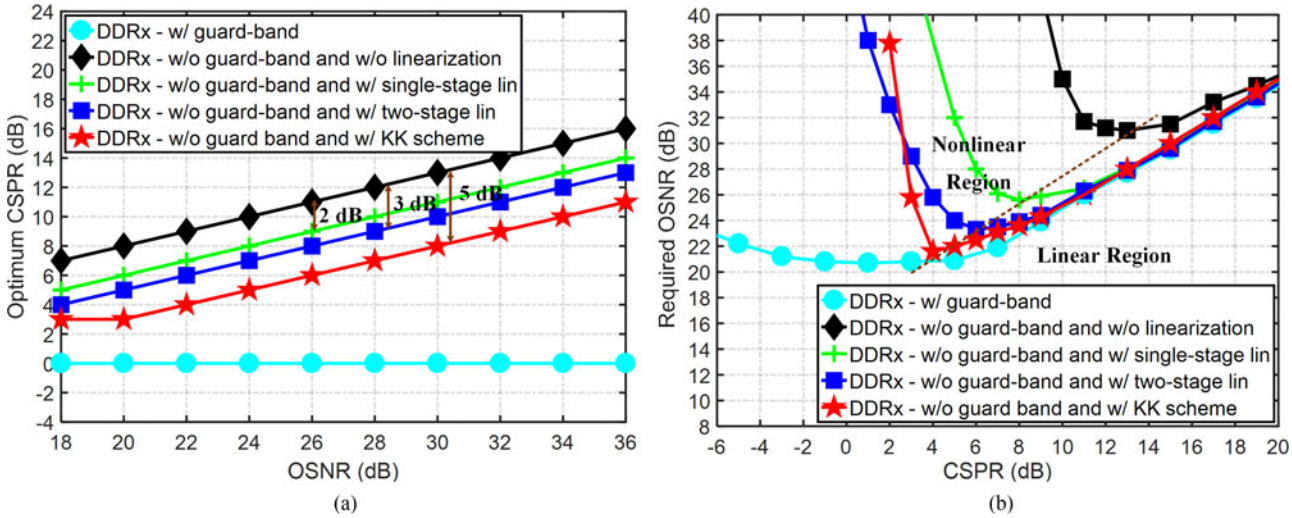

Fig. 6. (a) Theoretical optimum CSPR versus OSNR with different DD transceiver architectures. (b) Theoretical required OSNR (assuming $\mathrm{BER} = 3.8 \times 10^{-3}$) versus CSPR with different DD transceiver architectures.

the linear distortion due to SSBI is high at low CSPR values. However, since ASE noise dominates when the OSNR is low, SSBI is less critical and the optimum CSPR is low. As the OSNR increases, the impact of ASE noise reduces in comparison to that of SSBI, resulting in increasing optimum CSPR. Moreover, at a given value of OSNR, the optimum CSPR value is reduced by 2 dB to obtain the maximum compensation gain with the single-stage linearization filter and by 3 dB with the two-stage linearization filter, compared to the case without linearization. For the KK receiver, the optimum CSPR value is reduced by 5 dB over the OSNR range 20 dB to 36 dB, below which it is constant at the value of 3 dB, due to the requirement for minimum phase signaling. In the case of the single-photodiode DD system with spectral guard-band, the optimum CSPR remains at 0 dB for all the OSNR levels, which matches with the finding in [37]. The sensitivity of the system performance to CSPR, and the reductions in optimum CSPR achieved by implementing different SSBI compensation schemes are further presented in Fig. 6(b). Since the linearization DSP significantly reduces the impact of SSBI, the optimum CSPR value is significantly reduced in these cases. Due to its enhanced effectiveness in suppressing SSBI, the two-stage linearization filter provides greater reduction in the optimum CSPR compared with the single-stage linearization filter. The KK scheme achieves the biggest reduction in the optimum CSPR, though its performance is dramatically degraded at CSPR values below the optimum level (<4 dB) due to the minimum phase condition not being met.

IV. Experimental Setup

In order to assess the performance of DD transceivers with the three digital linearization approaches described in the previous sections, transmission experiments were carried out using the setup shown in Fig. 7. The optical transmission test-bed consisted of a 4 × 112 Gb/s SSB 16-QAM Nyquist-SCM transmitter, a straight-line standard single-mode fiber (SSMF) link and an optical bandpass filter (OBPF) followed by a single photodiode-based direct-detection receiver to select and recover the channel of interest.

At the transmitter, two high-speed arbitrary-waveform generators (Keysight M8196A AWG) operating at a sampling rate of 92 GSa/s and with 33 GHz 3-dB bandwidth were used to drive each IQ-modulator. The I- and Q- components of the SSB 16-QAM Nyquist-SCM signals were generated offline using MATLAB, and uploaded to the AWGs to serve as the IQ-modulators' driving signals. The modulation DSP generating the SSB Nyquist-SCM signal is described in detail in [23]. Four 2^{15} de Bruijn binary sequences were encoded onto a 16-QAM signal at 112 Gb/s (a symbol rate (f_s) of 28 GBd). A pair of root-raised cosine (RRC) filters with a roll-off factor (β) of 0.01 were utilized to carry out Nyquist pulse shaping on the I- and Q- components of the signal. The filtered components were up-converted to a subcarrier frequency of 14.28 GHz ($f_{sc} = 0.51 \cdot f_s$) and added to each other to obtain a DSB Nyquist-SCM signal. The subcarrier frequency and β were selected such that the spectral guard-band between the signal and the optical carrier was negligible. Following this, the lower frequency sideband was removed using a digital Hilbert transform sideband filter to generate a SSB 16-QAM Nyquist-SCM signal.

Four external cavity lasers (ECLs) operating at wavelengths around 1550 nm with 100 kHz linewidth were utilized as the transmitter optical sources. After passing through two IQ-modulators which were biased to achieve the desired optical carrier power, the modulated odd and even channels were multiplexed to generate the $4 \times 112\,\mathrm{Gb/s}$ WDM signal. By wavelength tuning the transmitter lasers, the WDM channel spacing was varied and the system performance was tested at three different values: 50, 37.5 and 35 GHz, corresponding to gross optical ISDs of 2.2, 3.0 and 3.2 (b/s)/Hz, respectively. The insets (I–III) of Fig. 7 show the optical WDM spectra, measured with an optical spectrum analyzer (OSA) at a resolution of 0.01 nm. Since the optimization of the CSPR is crucial to achieve

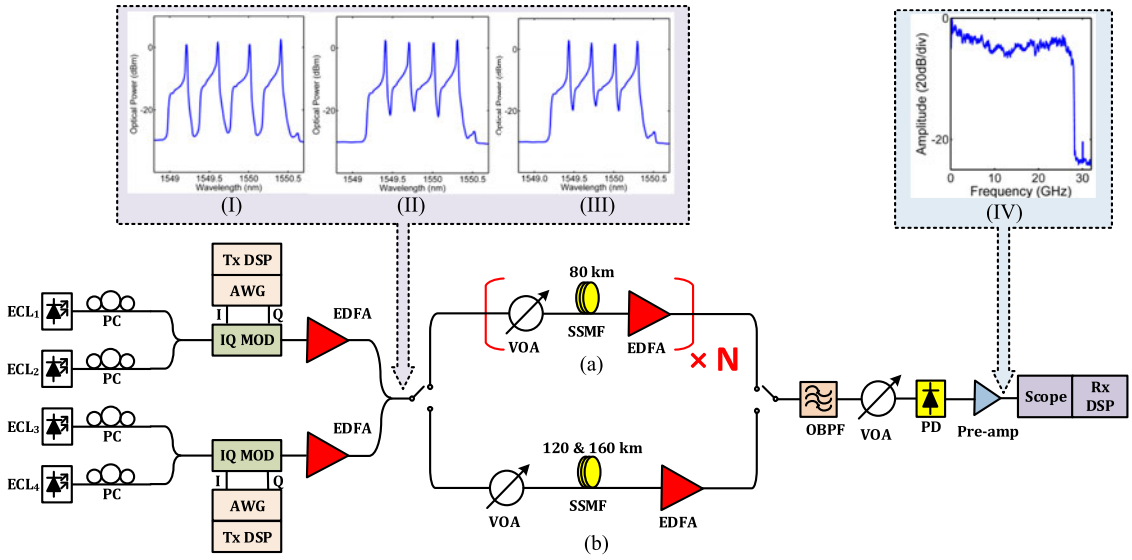

ECL: External cavity laser, AWG: Arbitrary-waveform generator, PC: Polarization controller, EDFA: Erbium-doped fiber amplifier, VOA: Variable optical attenuator, SSMF: Standard single mode fiber, OBPF: Optical Band-pass filter, PD: Photodiode.

Fig. 7. Experimental test-bed for 4 × 112 Gb/s WDM DD SSB 16-QAM Nyquist-SCM transmission with (a) multiple-span and (b) extended-reach single-span transmission link structures. Insets: WDM signal spectra with (I) 50 GHz, (II) 37.5 GHz and (III) 35 GHz channel spacing; (IV) detected digital signal spectrum.

the optimum performance in DD systems, as discussed in the previous sections, in the experiment, the optical carrier was obtained by biasing the IQ-modulators above the null point and the biases were adjusted to obtain the desired CSPR. The amplitude of the time-varying component of the drive signals was set sufficiently low to avoid significant penalty due to modulator nonlinearity.

Two transmission scenarios were assessed: firstly, straight-line multiple span fiber links, consisting of 80 km SSMF spans with inline erbium-doped fiber amplifiers (EDFAs), and, secondly, single-span fiber links with reaches of 120 km and 160 km, without mid-span amplification, and with an EDFA at the receiver. The noise figure of all EDFAs was 5 dB.

At the receiver, an OBPF (Yenista Optics XTM50-Ultrafine) with an adjustable bandwidth was used to demultiplex the channel of interest and remove the out-of-band ASE noise. The 3-dB bandwidth of the filter was set to 32 GHz for optimum system performance. The filtered signal was then detected using a single PIN photodiode, pre-amplified and digitized by a single ADC (Agilent DSA-X 96204Q) operating at 80 GSa/s. The received digital spectrum is plotted in the inset (IV) of Fig. 7. In the receiver DSP, following normalization and DC offset removal, the aforementioned linearization techniques were applied. Since effective linearization offers the possibility of performing digital compensation of linear optical effects at the receiver with near ideal performance [14], receiver-based electronic dispersion compensation (Rx-EDC) [38], was utilized to compensate the accumulated chromatic dispersion of the link. In contrast to transmitter-based EDC, the utilization of Rx-EDC simplifies the system operation since knowledge of link dispersion is not required at the transmitter. As described in [14], the difference in performance between Tx- and Rx-EDC depends on the effectiveness of the linearization scheme that is used. They can achieve similar performance if the beating interference is effectively suppressed. In the demodulation DSP (DEMOD DSP), frequency down-conversion and matched filtering with a RRC filter ($\beta = 0.01$) were applied. A 5-tap single-input-single-output filter, whose taps weights were updated using the least-mean square algorithm, was used for symbol re-timing. For fast convergence, initially, the cost function was set to a constant modulus. After convergence, the cost function was switched to decision-directed mode to recover the symbols. Finally, the signal was demodulated and the BER and error-vector-magnitude (EVM) [39] were calculated, the former by error counting over 2^{18} bits (corresponding to two repetitions of the de Bruijn sequences). For BER values between 10^{-4} and 10^{-5}, ten individual waveforms were captured and BER obtained from error counting, to ensure a sufficiently high confidence level.

V. Experimental Results

Both the optical back-to-back and WDM transmission evaluations were carried out with the experimental test-bed described in Section IV. System performance with a range of WDM channel spacing values, transmitting over the different link structures is presented in this section.

A. WDM Back-to-Back Performance Evaluation

Initially, the optical back-to-back performance was evaluated by performing ASE-noise loading at the receiver, with the experimental results plotted in Figs. 8 and 9.

To determine the minimum WDM channel spacing to achieve the highest possible ISD, initially, the channel spacing was varied from 33 to 50 GHz and the required OSNR at the HD-FEC BER threshold of 3.8×10^{-3} was monitored without using

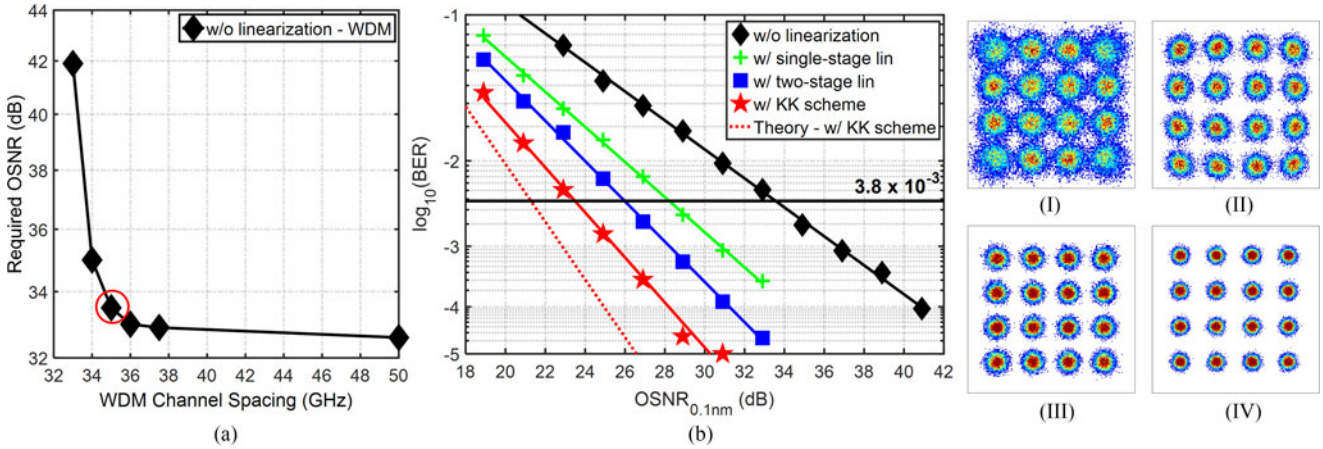

Fig. 8. (a) Required OSNR at BER $= 3.8 \times 10^{-3}$ versus WDM channel spacing without digital linearization. (b) BER versus OSNR at 35 GHz WDM channel spacing without and with different digital linearization schemes. Insets: Back-to-back received constellation diagrams at the OSNR of 31 dB, (I) without (20.4%), and with (II) single-stage linearization filter (14.7%), (III) two-stage linearization filter (12.9%), and (IV) KK scheme (9.7%).

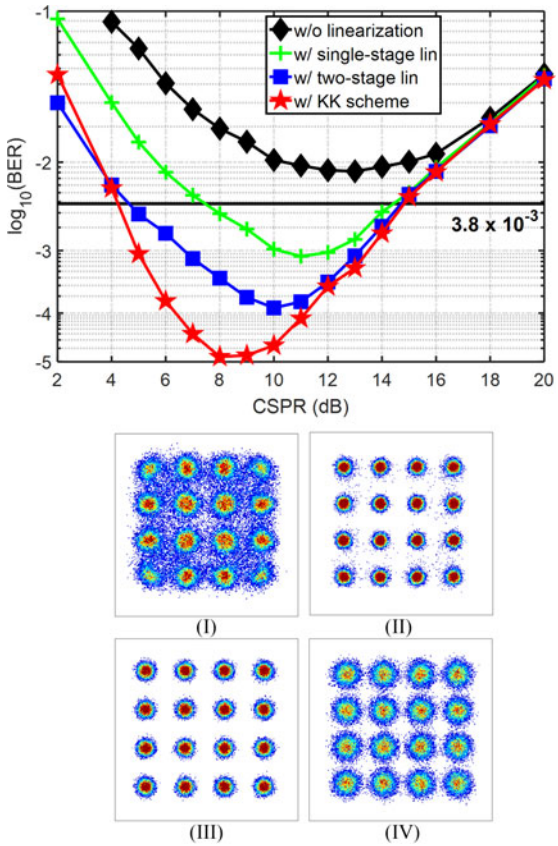

Fig. 9. (a) BER versus CSPR at 35 GHz WDM channel spacing without and with different digital linearization schemes at OSNR = 31 dB. Insets: back-to-back received constellation diagrams at (I) 2 dB (19.9%), (II) 5 dB (10.4%), (III) 8 dB (9.7%), and (IV) 14 dB (16.4%) CSPR with the KK scheme.

SSBI compensation [see Fig. 8(a)]. In order to maintain the linear crosstalk penalty caused by neighbouring channel at less than 1 dB, the minimum WDM channel spacing was found to be 35 GHz, yielding a gross ISD of 3.2 (b/s)/Hz. At a channel spacing of 35 GHz, BER versus OSNR for the cases without and with the different digital linearization techniques described in Section II, namely single-stage and two-stage linearization filters, and the KK scheme, is plotted in Fig. 8(b). The optimum performance was achieved by sweeping the CSPR from 2 dB to 16 dB and setting it to the optimum value for each OSNR level. It can be seen that the required OSNR at the HD-FEC threshold was 33.5 dB without linearization, reducing to 28.1 dB (a 5.4 dB improvement) by applying the single-stage linearization filter, and further reducing to 25.9 dB (a reduction of 7.6 dB) with the two-stage linearization filter. By utilizing the KK scheme (operating at 6 Sa/symbol), the required OSNR was reduced by 9.7 dB to 23.8 dB, showing that the KK scheme provides the best performance of all the techniques being compared. The difference in required OSNR values between the experiment (23.8 dB) and the simulated ideal system (21.5 dB), as presented in the previous section, is due to a number of factors: (i) the electrical noise introduced by the transceiver, including DAC and ADC quantization noise, (ii) the low-pass filtering and nonlinear characteristics of the electrical and optoelectronic components used in the experiment and (iii) the linear crosstalk from the adjacent 35 GHz-spaced channels (which contributed approximately 1 dB to the required OSNR). To observe the effectiveness of the compensation using these linearization approaches, the received signal constellations at an OSNR of 31 dB are presented in the insets of Fig. 8, with the corresponding EVMs listed in the caption.

The measured BER versus CSPR at 31 dB OSNR is plotted in Fig. 9, showing the sensitivity of the systems to the applied CSPR. Due to their increasing effectiveness in suppressing the SSBI, the optimum CSPR value was found to be reduced by approximately 2 dB, 3 dB and 5 dB using the single-stage, two-stage linearization filters and the KK scheme respectively, compared to the case without linearization. This finding matches well with the simulation results in Section III (see Fig. 6). The performance of the KK scheme operating at different CSPR values can also be assessed from the received signal constellations at this OSNR level, shown in Fig. 9. At lower CSPRs, since the minimum phase condition is not met, the KK scheme's performance is dramatically degraded.

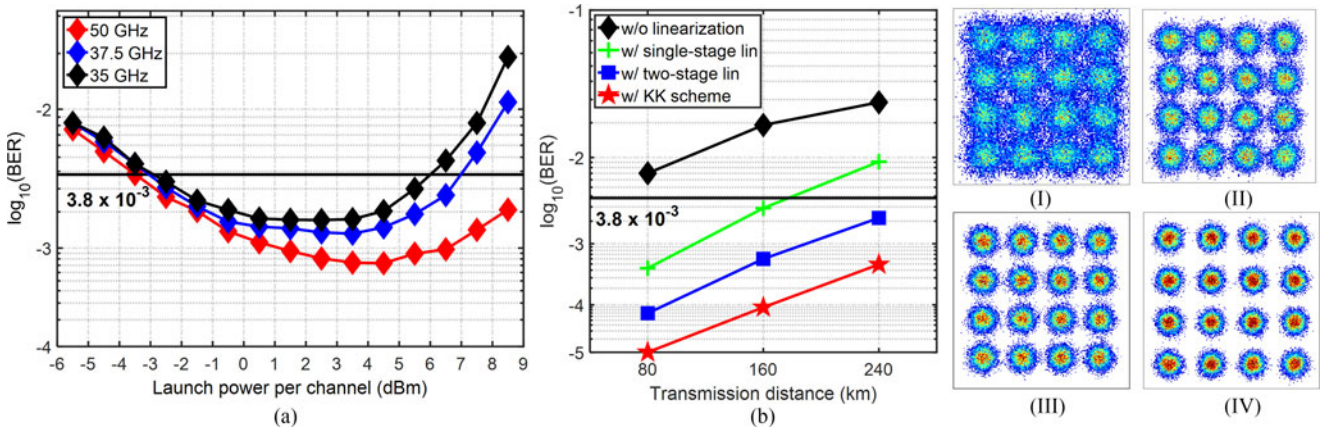

Fig. 10. (a) BER versus optical launch power per channel without linearization at different WDM channel spacing over 80 km WDM transmission. (b) BER versus transmission at 35 GHz WDM channel spacing without and with different digital linearization schemes. Insets: received constellation diagrams over 240 km WDM transmission, (I) without (23.4%), and with (II) single-stage linearization filter (19.0%), (III) two-stage linearization filter (16.0%), and (IV) the KK scheme (13.1%).

B. WDM Transmission Performance Evaluation

Following the optical back-to-back measurements, the system performance was assessed in experimental WDM transmission over both the multiple span and the extended single span fiber links.

1) Transmission With Multiple Span Fiber Links: In the transmission experiments with the multiple span links, the performance with different values of WDM channel spacing (50 GHz, 37.5 GHz and 35 GHz) over 80 km transmission was first investigated by measuring BER versus optical launch power per channel [see Fig. 10(a)]. It can be seen that the reduction in channel spacing not only increases the linear neighbouring channel crosstalk, but also increases the distortion due to fiber nonlinearity. Thus, a reduction in the optimum launch power by 2 dB was observed when reducing the channel spacing from 50 to 35 GHz. The BER (at the optimum launch power and CSPR) versus transmission distance over distances from 80 km to 240 km without and with digital linearization is plotted for the case of 35 GHz channel spacing in Fig. 10(b). It can be observed that the WDM transmission performance was significantly improved at all distances, with the BER at 240 km being decreased from 2.9×10^{-2} to 9.0×10^{-3} using the single-stage linearization filter, and further reducing to 2.1×10^{-3} and 5.5×10^{-4} with two-stage linearization filter and the KK scheme, respectively. The reach was enhanced by more than 200% (from less than 80 km to more than 240 km) by using either the two-stage linearization filter or the KK scheme. The corresponding received signal constellations at 240 km are presented in the insets, with the associated EVM values listed in the caption.

The performance of all four WDM channels at 35 GHz WDM channel spacing at a distance of 240 km (3 spans) is shown in Fig. 11. The average BER for all the channels was decreased from 2.7×10^{-2} without linearization, to 1.9×10^{-3} and 5.2×10^{-4} using the two-stage linearization filter and the KK scheme, respectively. Assuming the standard 7% HD-FEC overhead, the net ISD was 2.99 (b/s)/Hz. Considering the theoretical hard-decision decoding bound for the binary symmetric

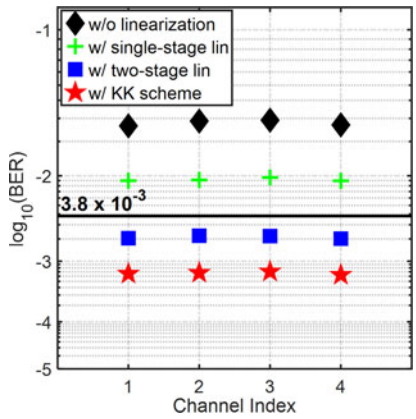

Fig. 11. BER for each received WDM channel at 35 GHz WDM channel spacing without and with different digital linearization schemes over 240 km WDM transmission.

channel [40] at the BER (p_b) of 5.2×10^{-4}, with the maximum code rate (r) given by:

$$r = 1 + p_b \cdot \log_2 p_b + (1 - p_b) \cdot \log_2 (1 - p_b) \qquad (1)$$

the value of r is 0.993, hence the theoretical upper bounds on the net bit rate per channel and net optical ISD are 111.3 Gb/s, and 3.18 (b/s)/Hz respectively.

2) Transmission With Extended-Reach Single-Span Fiber Links

The WDM transmission performance was next investigated for extended-reach fiber links without mid-span amplification, with 35 GHz WDM channel spacing. The BER versus optical launch power per channel in the 120 km and 160 km extended-reach single-span transmission scenarios are plotted in Fig. 12. Extending the length of a single span significantly reduces the OSNR at the receiver, and it can be observed that the minimum BERs at the optimum launch power per channel for 120 km transmission were higher, at 1.6×10^{-3} and 6.1×10^{-4} using the two-stage linearization filter and the KK

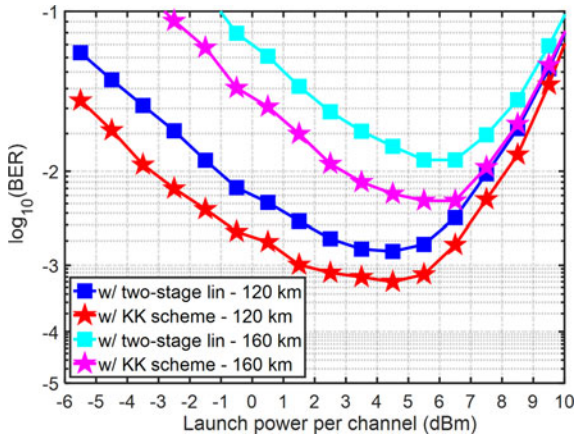

Fig. 12. BER versus optical launch power per channel at 35 GHz WDM channel spacing with different digital linearization schemes over extended reach single span fiber transmission of 120 and 160 km.

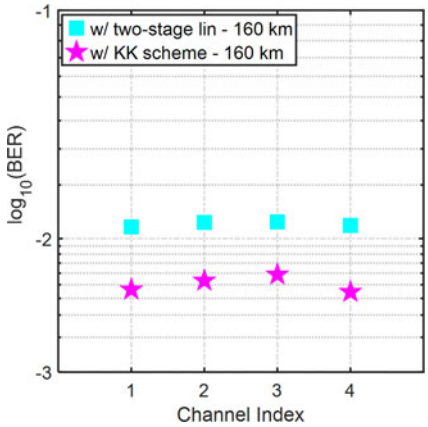

Fig. 13. BER for each received WDM channel at 35 GHz WDM channel spacing without and with different digital linearization schemes over extended reach single span fiber transmission of 160 km.

scheme respectively. After transmission over 160 km, the minimum BERs were 1.3×10^{-2} and 5.4×10^{-3} after applying these two schemes. Moreover, the optimum launch powers per channel were increased to 4.5 dB·m and 6.5 dB·m for 120 km and 160 km, respectively. Finally, the transmission performance of all four WDM channels over the 160 km extended-reach single-span link was measured, and is plotted in Fig. 13. Using the KK scheme, the average BER across all the WDM channels was 5.0×10^{-3}. The highest net optical ISD achievable in this case, assuming the theoretical hard-decision decoding bound for the binary symmetric channel, given by Eq. (1), was found to be 3.05 (b/s)/Hz.

These experimental results indicate that DD transceivers are capable of supporting high capacity (112 Gb/s/λ) and spectrally-efficient (net optical ISD above 3 (b/s)/Hz) wavelength division multiplexed transmission over the range of distances typically found in metropolitan area networks.

VI. Conclusions

We reported theoretical and experimental assessments of single-polarization direct-detection (DD) transceiver designs, using digital and optical linearization techniques, for 100 Gb/s/λ spectrally-efficient WDM metro networking. Initially, different coherent and DD transceiver structures were compared, based on simulations of ideal systems. The beating interference cancellation receiver (BICRx) was found to offer the best performance of the direct detection systems, but this is achieved at the expense of higher optical hardware complexity in the receiver. Digital linearization offers a good compromise between performance and complexity. The simulation results indicate that the Kramers-Kronig receiver has a required OSNR at the HD-FEC threshold (BER $= 3.8 \times 10^{-3}$) only 3.3 dB higher than that of the heterodyne coherent receiver. The difference in required OSNR between KK DD receiver and coherent heterodyne arises from the requirement for an optical carrier in the DD scheme, the power of which is included in the OSNR calculation. Following the simulation-based study, the performance of single photodiode-based DD systems was experimentally investigated using a 4×112 Gb/s WDM single-sideband (SSB) 16-QAM 0.51-cycle Nyquist subcarrier modulation (Nyquist-SCM) system, applying a variety of digital linearization schemes (single- and two-stage linearization filters and the Kramers-Kronig scheme), a range of WDM channel spacing values (from 35 to 50 GHz) and different transmission link structures (straight-line multiple-span links of up to 240 km and extended reach single-span links of up to 160 km, all using uncompensated standard SMF). The experimental results showed that digital linearization enables 35 GHz-spaced 112 Gb/s-per-channel single-polarization, single-photodetector direct-detection transmission at net optical ISDs exceeding 3 (b/s)/Hz over all these links. This technology can provide a potential solution for high capacity and spectrally-efficient WDM (100 Gb/s/λ and beyond) links for future metro networks.

References

[1] *Bell Labs Metro Network Traffic Growth: Architecture Impact Study*, Alcatel-Lucent, Boulogne-Billancourt, France, Strategic White Paper, 2013.

[2] *100 G Metro Transformation*, Fujitsu, Tokyo, Japan, Lightw. White Paper, 2014.

[3] D. Che, Q. Hu, and W. Shieh, "Linearization of direct detection optical channels using self-coherent subsystems," *J. Lightw. Technol.*, vol. 34, no. 2, pp. 516–524, Jan. 2016.

[4] R. I. Killey *et al.*, "Spectrally-efficient direct-detection WDM transmission system," in *Proc. 17th Int. Conf. Transp. Opt. Netw.*, 2015, Paper no. We.B3.2.

[5] W. R. Peng, I. Morita, and H. Tanaka, "Enabling high capacity direct-detection optical OFDM transmissions using beat interference cancellation receiver," in *Proc. 36th Eur. Conf. Exhib. Opt. Commun.*, 2010, Paper no. Tu.4.A.2.

[6] S. A. Nezamalhosseini, L. R. Chen, Q. Zhuge, M. Malekiha, F. Marvasti, and D. V. Plant, "Theoretical and experimental investigation of direct detection optical OFDM transmission using beat interference cancellation receiver," *Opt. Express*, vol. 21, no. 13, pp. 15237–15246, 2013.

[7] B. J. C. Schmidt, A. J. Lowery, and L. B. Du, "Low sample rate transmitter for direct-detection optical OFDM," in *Proc. Conf. Opt. Fiber Commun.*, 2009, Paper no. OWM4.

[8] L. Zhang, T. Zuo, Q. Zhang, J. Zhou, E. Zhou, and G. N. Liu, "150-Gb/s DMT over 80-km SMF transmission based on spectrally efficient SSBI cancellation using guard-band twin-SSB technique," in *Proc. Eur. Conf. Opt. Commun.*, 2016, pp. 1178–1180.

[9] S. Randel, D. Pilori, S. Chandrasekhar, G. Raybon, and P. Winzer, "100-Gb/s discrete-multitone transmission over 80-km SSMF using single-sideband modulation with novel interference-cancellation scheme," in *Proc. Eur. Conf. Opt. Commun.*, 2015, Paper no. Mo.4.5.2.

[10] Z. Li *et al.*, "Two-stage linearization filter for direct-detection subcarrier modulation," *IEEE Photon. Technol. Lett.*, vol. 28, no. 24, pp. 2838–2841, Dec. 2016.
[11] Z. Li *et al.*, "112 Gb/s/λ WDM direct-detection Nyquist-SCM transmission at 3.15 (b/s)/Hz over 240 km SSMF enabled by novel beating interference compensation," in *Proc. Conf. Opt. Fiber Commun.*, 2017, Paper no. Tu3I.4.
[12] A. Mecozzi, C. Antonelli, and M. Shtaif, "Kramers-Kronig coherent receiver," *Optica*, vol. 3, no. 11, pp. 1220–1227, 2016.
[13] C. Antonelli, A. Mecozzi, and M. Shtaif, "Kramers-Kronig PAM transceiver," in *Proc. Conf. Opt. Fiber Commun.*, 2017, Paper no. Tu3I.5.
[14] Z. Li *et al.*, "SSBI mitigation and Kramer-Kronig scheme in single-sideband direct-detection transmission with receiver-based electronic dispersion compensation," *J. Lightw. Technol.*, vol. 35, no. 10, pp. 1887–1893, May 2017.
[15] Z. Li *et al.*, "Joint optimization of resampling rate and carrier-to-signal power ratio in direct-detection Kramers-Kronig receivers," in *Proc. Eur. Conf. Opt. Commun.*, 2017, Paper no. W.2.D.3.
[16] X. Chen *et al.*, "218-Gb/s single-wavelength, single-polarization, single-photodiode transmission over 125-km of standard single-mode fiber using Kramers-Kronig detection," in *Proc. Conf. Opt. Fiber Commun.*, 2017, Paper no. Th5B.6.
[17] X. Chen *et al.*, "4 × 240 Gb/s dense WDM and PDM Kramers-Kronig detection with 125-km SSMF transmission," in *Proc. Eur. Conf. Opt. Commun.*, 2017, Paper no. W.2.D.4.
[18] S. Fan *et al.*, "Twin-SSB direct detection transmission over 80 km SSMF using Kramers-Kronig receiver," in *Proc. Eur. Conf. Opt. Commun.*, 2017, Paper no. W.2.D.5.
[19] Z. Li *et al.*, "168 Gb/s/λ direct-detection 64-QAM SSB Nyquist-SCM transmission over 80 km uncompensated SSMF at 4.54 b/s/Hz net ISD using a Kramers-Kronig receiver," in *Proc. Eur. Conf. Opt. Commun.*, 2017, Paper no. Tu.2.E.1.
[20] Z. Li *et al.*, "Reach enhancement for WDM direct-detection subcarrier modulation using low-complexity two-stage signal-signal beat interference cancellation," in *Proc. Eur. Conf. Opt. Commun.*, 2016, Paper no. M 2.B.1.
[21] K. Zou, Y. Zhu, F. Zhang, and Z. Chen, "Spectrally efficient terabit optical transmission with Nyquist 64-QAM half-cycle subcarrier modulation and direct-detection," *Opt. Lett.*, vol. 41, no. 12, pp. 2767–2770, 2016.
[22] W. Peng *et al.*, "Spectrally efficient direct-detected OFDM transmission employing an iterative estimation and cancellation technique," *Opt. Express*, vol. 17, no. 11, pp. 9099–9111, 2009.
[23] Z. Li *et al.*, "Signal-signal beat interference cancellation in spectrally-efficient WDM direct-detection Nyquist-pulse-shaped 16-QAM subcarrier modulation," *Opt. Express*, vol. 23, no. 18, pp. 23694–23709, 2015.
[24] C. Sánchez, B. Ortega, and J. Capmany, "System performance enhancement with pre-distorted OOFDM signal waveforms in IM/DD systems," *Opt. Express*, vol. 22, no. 6, pp. 7269–7283, 2014.
[25] C. Ju, X. Chen, N. Liu, and L. Wang, "SSII cancellation in 40 Gbps VSB-IMDD OFDM system based on symbol pre-distortion," in *Proc. Eur. Conf. Opt. Commun.*, 2014, Paper no. P.7.9.
[26] Z. Li, M. S. Erkilinc, R. Bouziane, B. C. Thomsen, P. Bayvel, and R. I. Killey, "Simplified DSP-based signal-signal beat interference mitigation technique for direct detection OFDM," *J. Lightw. Technol.*, vol. 34, no. 3, pp. 866–872, Feb. 2016.
[27] Z. Li *et al.*, "Comparison of digital signal-signal beat interference compensation techniques in direct-detection subcarrier modulation systems," *Opt. Express*, vol. 24, no. 25, pp. 29176–29189, 2016.
[28] K. Kikuchi, "Fundamentals of coherent optical fiber communications," *J. Lightw. Technol.*, vol. 34, no. 1, pp. 157–179, Jan. 2016.
[29] E. Ip, A. P. T. Lau, D. J. F . Barros, and J. M. Kahn, "Coherent detection in optical fiber systems," *Opt. Express*, vol. 16, no. 2, pp. 753–791, 2008.
[30] A. O. Wiberg, B.-E. Olsson, and P. A. Andrekson, "Single cycle subcarrier modulation," in *Proc. Conf. Opt. Fiber Commun.*, 2009, Paper no. OTuE.1.
[31] J. C. Cartledge and A. S. Karar, "100 Gb/s intensity modulation and direct detection," *J. Lightw. Technol.*, vol. 32, no. 16, pp. 2809–2814, Aug. 2014.
[32] K. Zou, Y. Zhu, and F. Zhang, "800 Gb/s (8 × 100 Gb/s) Nyquist half-cycle single sideband modulation direct detection transmission over 320 km SSMF," *J. Lightw. Technol.*, vol. 35, no. 10, pp. 1900–1905, May 2017.
[33] Y. Gao, J. C. Cartledge, A. S. Kashi, S. S.-H. Yam, and Y. Matsui, "Direct modulation of a laser using 112 Gb/s 16-QAM Nyquist subcarrier modulation," *IEEE Photon. Technol. Lett.*, vol. 29, no. 1, pp. 35–38, Jan. 2017.
[34] K. Zhong *et al.*, "Experimental demonstration of 608 Gbit/s short reach transmission employing half-cycle 16QAM Nyquist-SCM signal and direct detection with 25 Gbps EML," *Opt. Express*, vol. 24, no. 22, pp. 25057–25067, 2016.
[35] H. Voelcker, "Demodulation of single-sideband signals via envelope detection," *IEEE Trans. Commun. Technol.* vol. COM-14, no. 1, pp. 22–30, Feb. 1966.
[36] K. Roberts, D. Beckett, D. Boertjes, J. Berthold, and C. Laperle, "100 G and beyond with digital coherent signal processing," *IEEE Commun. Mag.*, vol. 48, no. 7, pp. 62–69, Jul. 2010.
[37] A. J. Lowery, L. B. Du, and J. Armstrong, "Performance of optical OFDM in ultralong-haul WDM lightwave systems," *J. Lightw. Technol.*, vol. 25, no. 1, pp. 131–138, Jan. 2007.
[38] M. Sieben, J. Conradi, and D. E. Dodds, "Optical single sideband transmission at 10 Gb/s using only electrical dispersion compensation," *J. Lightw. Technol.*, vol. 17, no. 10, pp. 1742–1749, Oct. 1999.
[39] R. A. Shafik, M. S. Rahman, and A. R. Islam, "On the extended relationships among EVM, BER and SNR as performance metrics," in *Proc. Int. Conf. Elect. Comput. Eng.*, 2006, pp. 408–411.
[40] C. E. Shannon, "A mathematical theory of communication," *Bell Syst. Tech. J.* vol. 27, no. 3, pp. 379–423, 1948.

Authors' biographies not available at the time of publication.